Optimization of Attosecond Pulse Generation

Y. Mairesse,[1] A. de Bohan,[1] L. J. Frasinski,[2] H. Merdji,[1] L. C. Dinu,[3] P. Monchicourt,[1] P. Breger,[1] M. Kovačev,[1] T. Auguste,[1] B. Carré,[1] H. G. Muller,[3] P. Agostini,[1] and P. Salières[1]

[1]*CEA/DSM/DRECAM/SPAM, bât. 522, Centre d'Etudes de Saclay, 91191 Gif-sur-Yvette, France*

[2]*The University of Reading, J. J. Thomson Physical Laboratory, Whiteknights, P.O. Box 220, Reading RG6 6AF, United Kingdom*

[3]*FOM-Institute for Atomic and Molecular Physics, Kruislaan 407, 1098 SJ Amsterdam, Netherlands*

(Received 3 May 2004; published 13 October 2004)

The generation of attosecond pulses by superposition of high harmonics relies on their synchronization in the emission. Our experiments in the low-order, plateau, and cutoff regions of the spectrum reveal different regimes in the electron dynamics determining the synchronization quality. The shortest pulses are obtained by combining a spectral filtering of harmonics from the end of the plateau and the cutoff, and a far-field spatial filtering that selects a single electron quantum path contribution to the emission. This method applies to isolated pulses as well as pulse trains.

DOI: 10.1103/PhysRevLett.93.163901 PACS numbers: 42.65.Ky, 32.80.Wr, 42.65.Re

The strongly nonlinear interaction taking place when an intense infrared (IR) laser pulse is focused into a rare gas jet results in the coherent emission of extreme ultraviolet (XUV) light [1] with a characteristic spectrum showing a plateau and a sharp cutoff at high energy [2]. This process offers the unique opportunity of generating attosecond pulses, as recently demonstrated by two techniques. First, starting from a few-cycle laser pulse, the highest energy photons are only emitted at the maximum of the laser envelope. The cutoff is then continuous and by spectrally selecting it, one can obtain a single pulse of 250 as duration [3,4]. Second, using a multicycle IR pulse provides a discrete spectrum containing only odd harmonics of the laser frequency. Selecting many harmonics in the plateau results in emission of XUV bursts every half laser period, forming an attosecond pulse train (APT) whose wagons can be as short as 130 as [5,6]. In both cases, the condition for the production of short pulses is a near-linear spectral phase of the XUV radiation. For a discrete spectrum, this means that harmonics must be phase-locked, i.e., synchronized. The phase-locking of harmonics is closely related to the electronic dynamics in the generation process. In the semiclassical "three-step" model [7,8], part of the electron wave packet first tunnels out of the atomic potential lowered by the laser field; it is then driven by the strong IR field in the continuum; finally, it can recombine with the parent ion, emitting a XUV photon whose energy is given by the electron return kinetic energy. The recombination times of the different electron trajectories determine the emission times of the different XUV frequencies, and thus their synchronization.

Recent studies have stressed two main sources of asynchronism that raise important questions for the reliable generation of shorter pulses. First, each harmonic is associated to mainly two ("short" and "long") electron trajectories that have the same return energy but very different return times. The single-atom response thus consists of at least two bursts per half laser cycle, which blurs the attosecond structure. Fortunately, the short trajectory contribution can be macroscopically selected by adjusting carefully the phase matching conditions [9]: when the generating laser is focused slightly before the gas jet, the macroscopic temporal profile exhibits a "clean" APT with a single attosecond pulse per half cycle. However, the quality of the APT is predicted to depend critically on the focus/jet relative position [10]. Can we find robust generation conditions where phase-locking will be preserved? Second, even if a trajectory selection is achieved, the short trajectories associated to the different plateau harmonics have different recombination times [6]. This induces a quadratic term in the spectral phase, equivalent to a linear frequency chirp of the attosecond pulses, setting a lower limit to the XUV pulse duration achievable in given generation conditions. Is this chirp also present in the cutoff region, where the electron dynamics is more complex? This would prevent the generation of isolated pulses of 100 as duration.

In this Letter, we perform a thorough study of the phase-locking of high harmonics. We first investigate the influence of the focusing geometry on the generation process. We demonstrate that a good phase-locking can be robustly achieved through quantum path selection by spatially filtering the harmonic radiation. We then study the relative phase of harmonics over the full spectrum. We find that the low harmonics are temporally shifted in emission with respect to the following ones, while harmonics from the cutoff are fully phase-locked.

In our experiments, we performed measurements of the harmonic relative phases based on two-photon two-color photoionization [11], with the same setup as in [6]. Briefly, we use a 20 Hz, 45 fs, up-to-50 mJ, 800 nm laser system. The beam is split into two—outer and inner—components in a delay line. The outer annular part is focused with a lens of 1 m focal length and generates harmonics in a 1 mm thick neon gas jet. The peak laser

 © 2004 The American Physical Society

intensity is 4.7×10^{14} W/cm^2 and the confocal parameter $b = 23$ mm. The beam is then blocked by a 4 mm diaphragm placed 60 cm after the jet. The harmonic radiation that passes through this diaphragm is refocused by a 70 cm Pt coated toroidal mirror into a target helium jet, in the source volume of a photoelectron time-of-flight spectrometer. The inner circular part of the initial laser beam is focused into the second gas jet with an adjustable delay with respect to the harmonic beam. The photoelectron spectra show main harmonic lines and sidebands induced by the dressing IR beam. The phase of the sideband oscillations resulting from the delay scanning allows retrieving the phase difference between two consecutive harmonics.

For the phase-locking analysis, we select a group of ten harmonics (from 17 to 35) and reconstruct the corresponding APT from the measured amplitudes and spectral phases. The temporal profiles are presented in Fig. 1(a). They are normalized to contain the same energy (short duration is thus associated to high peak value). The

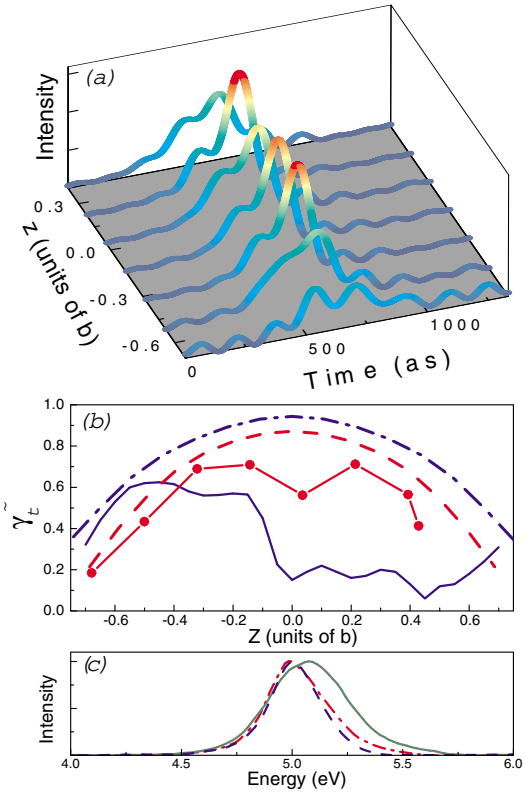

FIG. 1 (color online). (a) Measured (normalized) temporal profiles for 10 harmonics (17 to 35) generated in Ne at 4.7×10^{14} W/cm^2 (intensity at focus). (b) Normalized phase-locking parameters: measurements $\tilde{\gamma}_t^{\mathrm{exp}}$ (red dots) and simulations $\tilde{\gamma}_t^{\mathrm{sgl}}$ (red dashed line) at 4.7×10^{14} W/cm^2; TDSE calculations from [10] for harmonics 41 to 59 (blue line) and simulations $\tilde{\gamma}_t^{\mathrm{sgl}}$ (blue dashed-dotted line) at 6×10^{14} W/cm^2. (c) Measured normalized spectra for harmonic 19 at $z = -0.3b$ (red dashed dots), 0 (green line), and $0.2b$ (blue dashed line).

laser focusing appears as a crucial parameter for the production of short bursts. We always obtain a single burst per half period, but its shape dramatically depends on the position z of the focus with respect to the jet ($z > 0$ means focusing after the jet). Strongly distorted bursts are observed at large z, while nice pulses with a minimum duration of 130 as FWHM are measured when focusing slightly before or after the gas jet.

The temporal distortions of the attosecond pulses obtained by superposing N harmonics can be quantified by introducing the degree of phase-locking [10]

$$\gamma_t = \frac{\int_{\tau_N} dt I_{XUV}(t)}{\int_{T_0/2} dt I_{XUV}(t)}. \quad (1)$$

This factor represents the proportion of XUV energy emitted within $\tau_N = T_0/(2N)$ during half a laser period $T_0/2$. It can be normalized as $\tilde{\gamma}_t = (\gamma_t - 2\tau_N/T_0)/(\gamma_t^{FT} - 2\tau_N/T_0)$, where γ_t^{FT} is the value obtained in the case of perfect phase-locking [12]. Figure 1(b) shows the variation of $\tilde{\gamma}_t^{\mathrm{exp}}$ in our measurements. The phase-locking is good when z is between $-0.3b$ and $0.3b$ (even though it slightly decreases for $z = 0$), and deteriorates at large $|z|$. When z is larger than $0.4b$, the harmonic flux becomes too low to be measured. These results can be compared to the macroscopic simulations based on the resolution of the time-dependent Schrödinger equation (TDSE) [10] (blue line). The most striking feature is that the experimental curve is almost symmetric with respect to $z = 0$, in contrast with the TDSE calculations. In the latter, the very poor phase-locking obtained for $z > 0$ is due to the long quantum trajectories contributions that result in the appearance of many bursts per half cycle. This behavior was systematically observed when combining other harmonics or changing the intensity. On the measured temporal profiles, the absence of multiple bursts for $z > 0$ indicates that the contribution of a single trajectory is selected, even when the laser is focused in or after the jet. This selection is performed thanks to the diaphragm placed after the generating jet. Indeed, in the far-field, the harmonic wave front separates in two regions, due to the different phase characteristics of the two quantum paths: the short trajectory contribution is emitted on-axis, while the long one is much more divergent [13–16]. In our experiment, the far-field diaphragm therefore acts as a spatial filter that selects the contribution of the short trajectory. This is confirmed by the fact that the harmonic spectra (derived from the photoelectron spectra) obtained for $z > 0$ are very similar to the ones obtained for $z < 0$, without any broadening or pedestal as usually observed for the long quantum path [17] [Fig. 1(c)]. In parallel to this experiment, we have performed studies of the spatial profile of harmonic emission in the same focusing geometry [18]. They confirmed that a similar diaphragm aperture eliminates most of the long trajectory contribution.

However, the selection of the short quantum paths does not imply a perfect harmonic phase-locking: in the plateau, the attosecond pulses generated by the short quantum paths are positively chirped, while this chirp is negative for the long ones [6]. In the APT reconstructed from our measurements, the bursts always present a positive chirp (discussed below), which is consistent with the identification of the short trajectory. This chirp is inversely proportional to the generating laser intensity [6]. Consequently, it should increase when the focus is moved away from the gas jet, degrading phase-locking. We evaluated the intensity in the gas jet as a function of the focus position, and calculated the short-path single-atom phase-locking parameter $\tilde{\gamma}_t^{\mathrm{sgl}}$ [Fig. 1(b)]. The microscopic calculations are in good general agreement with the experiment, and explain the strong distortion of the APT at large z. The agreement is not so good when the laser is focused right in the jet. This can be explained by considering the harmonic spectrum obtained in $z = 0$ [Fig. 1(c)], that presents a clear blue shift indicating an important ionization of the generating medium [19]. Indeed, the laser intensity approaches the saturation intensity of neon; the phase-locking is then spoiled by propagation effects and no longer matches the single-atom prediction [6]. Note that the results obtained by Gaarde *et al.* also deviate from the corresponding $\tilde{\gamma}_t^{\mathrm{sgl}}$ curve when the intensity reaches 4×10^{14} W/cm^2 ($z = -0.4b$). In conclusion, the high sensitivity of phase-locking to the focusing geometry can be considerably reduced by spatially selecting the short quantum path contributions, resulting in a regular APT.

Even in optimized focusing conditions, the intrinsic lack of phase-locking in the plateau sets a limitation to the generation of short pulses. Hence, we now turn to the study of the harmonic phase-locking in the cutoff region.

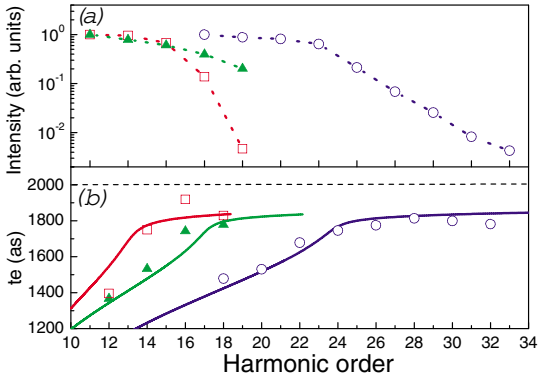

FIG. 2 (color online). Harmonic intensities (a) and emission times (b) obtained by generating in Xe (detection in Ar) at 3×10^{13} W/cm^2 (red squares) and 6×10^{13} W/cm^2 (green triangles), and by generating in Ar (detection in He) at 9×10^{13} W/cm^2 (blue circles). In (b), the solid lines are the short trajectory emission times given by the single-atom calculations, and the dashed line indicates the zero of the laser field.

Measurements are difficult here, due to the rapid decrease in harmonic flux. Figure 2 presents the results obtained by generating in xenon and argon at different laser intensities. We plot the emission time of harmonics (group delay), defined as $t_e(\omega_{q+1}) = \frac{\partial \phi}{\partial \omega}(\omega_{q+1}) \approx \frac{\phi_{q+2} - \phi_q}{2\omega_0}$, where ϕ_q is the average spectral phase of harmonic q and ω_0 the laser frequency. This representation allows both a clear visualization of the harmonic synchronization and a direct comparison with theory. Within the Feynman's path integral analysis of the harmonic emission [17], we calculated the complex recombination times of the electron with the parent ion. Their real part gives the harmonic emission times. Note that calculations in the complex plane are necessary to describe the cutoff, since this is a classically forbidden region. We obtain a good agreement between calculations and measurements [Fig. 2(b)]. In all cases, we observe the same behavior: in the plateau, t_e increases linearly with the order, leading to a positive linear chirp of the attosecond pulses, larger at low intensity. In the cutoff region, characterized by a sudden decrease of the harmonic intensity [see Fig. 2(a)], the emission time becomes independent of the harmonic order: the harmonics are perfectly phase-locked. Our measurement allows retrieving the absolute timing of harmonic emission with respect to the fundamental field [20]. Cutoff harmonics are found to be emitted 200 ± 50 as before the zero of the IR field.

These results can be discussed within the perspective of the generation of a single attosecond pulse by a few-cycle IR beam, through spectral selection of the cutoff radiation. In that case, our analysis is still valid (neglecting nonadiabatic effects), the difference being that the spectrum becomes continuous, as the process is no more periodic. The resulting attosecond pulse hence fulfills the properties illustrated above: it is Fourier-limited, and it is emitted before the zero of the IR field. The first point is essential for generating ultrashort pulses, and is consistent with the recent measurement of a close-to-Fourier-limit 250 as pulse [4]. Furthermore, the accurate knowledge of the synchronization of the XUV burst with the laser field provides an absolute time reference for their use in attosecond pump-probe spectroscopy.

The cutoff harmonics are interesting for the generation of very short pulses, but provide low XUV flux. In contrast, the low-frequency region of the spectrum could lead to the generation of intense APT, and thus needs to be characterized in terms of harmonic phase-locking. We performed measurements by generating in neon (ionization potential $Ip_{Ne} = 21.6$ eV $= 13.9\ \hbar\omega_0$) and detecting in argon ($Ip_{Ar} = 15.8$ eV $= 10.2\ \hbar\omega_0$), which allows detection of harmonics above H9. Figure 3 presents the harmonic emission times as a function of the order for several laser intensities. The general behavior is much less regular than in the plateau. The emission times corresponding to sidebands 12 and 14 are systematically

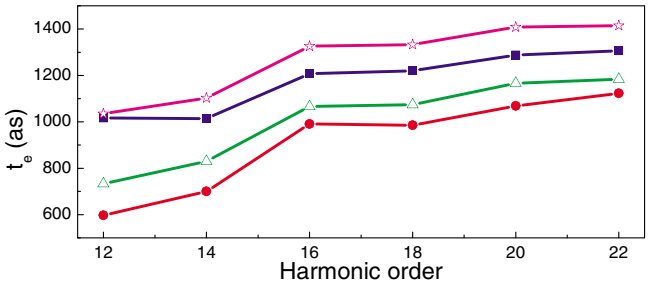

FIG. 3 (color online). Emission time of low-order harmonics generated in Ne (detection in Ar) at 2×10^{14} W/cm^2 (red circles), 3×10^{14} W/cm^2 (green triangles), 3.5×10^{14} W/cm^2 (blue squares), and 4×10^{14} W/cm^2 (magenta stars).

shifted with respect to the following ones. The shift decreases with increasing laser intensity, from about 300 as at 2×10^{14} W/cm^2 to less than 200 as at 3.5×10^{14} W/cm^2. We checked from two independent calculations that this shift was not an artifact due to the atomic phase terms in the sidebands oscillation [6]. The semiclassical calculations successfully used up to now predict that the lowest harmonics are more desynchronized than the plateau ones, with a smooth transition. However, this model is not expected to predict accurately the behavior of low-order harmonics. In particular, sidebands 12 and 14 involve harmonics whose energy is smaller than Ip_{Ne} and are thus classically forbidden in the "three-step" model. The observed shift could be the signature that the main generation mechanism is here a multiphoton process, where resonance effects become important. Such a time shift in the emission implies a temporal broadening of the attosecond pulses. Note that in the case of harmonic generation in xenon ($Ip_{Xe} = 12.1$ eV $= 7.8\ \hbar\omega_0$), a similar time shift may exist between emissions of harmonic seven and the following ones. This could explain the pulse duration longer than expected recently measured for the superposition of harmonics 7 to 15 generated in this gas [21].

In conclusion, the optimized conditions for the production of short attosecond pulses are generation at high enough laser intensity but below the saturation intensity and spectral selection of the end of the plateau and the cutoff region. Moreover, spatial selection of the short quantum path provides robust experimental conditions with respect to the laser focus/gas jet relative position. Such optimization should result in the generation of sub-100 as pulses with existing experimental setups.

We thank O. Gobert, P. Meynadier, and M. Perdrix for their support on the experiment, and M. B. Gaarde, S. Kazamias, and A. Maquet for fruitful discussions. This work was partially supported by the European Community's Human Potential Programme under Contracts No. HPRN-CT-2000-00133, ATTO, and No. HPRI-CT-2002-00191, SLIC. L. C. D. and H. G. M. are also funded by FOM/NWO and L. J. F. is partially supported by EPSRC GR/S22424/01.

[1] P. Salières, A. L'Huillier, Ph. Antoine, and M. Lewenstein, Adv. At. Mol. Opt. Phys. **41**, 83 (1999).
[2] M. Ferray, A. L'Huillier, X. F. Li, L. A. Lompré, G. Mainfray, and C. Manus, J. Phys. B **21**, L31 (1988).
[3] M. Hentschel *et al.*, Nature (London) **414**, 509 (2001).
[4] R. Kienberger *et al.*, Nature (London) **427**, 817 (2004).
[5] P. M. Paul, E. S. Toma, P. Breger, G. Mullot, F. Augé, Ph. Balcou, H. G. Muller, and P. Agostini, Science **292**, 1689 (2001).
[6] Y. Mairesse *et al.*, Science **302**, 1540 (2003).
[7] P. B. Corkum, Phys. Rev. Lett. **71**, 1994 (1993).
[8] K. J. Schafer, B. Yang, L. F. DiMauro, and K. C. Kulander, Phys. Rev. Lett. **70**, 1599 (1993).
[9] Ph. Antoine, A. L'Huillier, and M. Lewenstein, Phys. Rev. Lett. **77**, 1234 (1996).
[10] M. B. Gaarde and K. J. Schafer, Phys. Rev. Lett. **89**, 213901 (2002).
[11] V. Véniard, R. Taïeb, and A. Maquet, Phys. Rev. A **54**, 721 (1996).
[12] In [10], γ_t^{FT} is set to 0.775, which corresponds to equal harmonic amplitudes, while in our calculations we take the measured amplitudes into account. With the same convention as Gaarde *et al.*, the experimental curve is slightly shifted vertically, with a maximum $\tilde{\gamma}_t^{\exp} = 0.6$ at the saturation, which is in excellent agreement with their results.
[13] P. Salières, A. L'Huillier, and M. Lewenstein, Phys. Rev. Lett. **74**, 3776 (1995).
[14] M. Bellini, C. Lynga, A. Tozzi, M. B. Gaarde, T. W. Hänsch, A. L'Huillier, and C.-G. Wahlström, Phys. Rev. Lett. **81**, 297 (1998).
[15] C. Lynga, M. B. Gaarde, C. Delfin, M. Bellini, T. W. Hänsch, A. L'Huillier, and C.-G. Wahlström, Phys. Rev. A **60**, 4823 (1999).
[16] M. B. Gaarde, F. Salin, E. Constant, Ph. Balcou, K. J. Schafer, K. C. Kulander, and A. L'Huillier, Phys. Rev. A **59**, 1367 (1999).
[17] P. Salières *et al.*, Science **292**, 902 (2001).
[18] H. Merdji, M. Kovačev, P. Salières, and B. Carré (to be published).
[19] C. G. Wahlström, J. Larsson, A. Persson, T. Starczewski, S. Svanberg, P. Salières, Ph. Balcou, and A. L'Huillier, Phys. Rev. A **48**, 4709 (1993).
[20] L. C. Dinu *et al.*, Phys. Rev. Lett. **91**, 063901 (2003).
[21] P. Tzallas, D. Charalambidis, N. A. Papadogiannis, K. Witte, and G. D. Tsakiris, Nature (London) **426**, 267 (2003).